

Architectural Design for Multistage 2-D MEMS Optical Switches

Gangxiang Shen, *Member, IEEE*, Tee Hiang Cheng, *Member, IEEE*, Sanjay K. Bose, *Senior Member, IEEE*, Chao Lu, *Member, IEEE*, and Teck Yoong Chai

Abstract—Next-generation wavelength routing optical networks requiring optical cross connects (OXC) in the network have the ability to direct optical signals from any input interface to suitable output interfaces by configuring their internal embedded optical switch matrices. Microelectromechanical systems (MEMS) switches are regarded as the most promising technology to achieve such functionality. We consider the construction of a multistage MEMS switch network with single two-dimensional (2-D) MEMS switch blocks. A power loss model is developed that calls on a single MEMS block that is then used to develop the model for a three-stage Clos network. An effective model for maximum loss difference between calls is also developed. Based on these, the paper also proposes three connection patterns [Max + Min greedy (MMG), compressed extended generalized shuffle 1 (C-EGS-1), and compressed extended generalized shuffle 2 (C-EGS-2)] to connect outlet ports and inlet ports between two neighboring stages in a three-stage Clos network. These connection patterns are proved to be optimal and efficient enough to reach the minimums of both the maximum power loss of calls and the maximum loss difference between calls.

Index Terms—Clos network, connection pattern, maximum loss difference between calls, maximum power loss of calls, microelectromechanical system (MEMS), optical cross connect (OXC).

I. INTRODUCTION

OPTICAL switch is a crucial component for the next generation wavelength routing optical networks to achieve the functionalities of establishing, modifying, and releasing lightpath services on demand [1]–[3]. The currently available and researched technologies for this are micromechanical system (MEMS) switches [4]–[6], bubble-jet switches [7]–[9], liquid-crystal switches [10], [11], mechanical optical switches, thermo-optical switches [12], [13], and acousto-optical switches [14], [15]. Among them, MEMS switches, bubble-jet switches, and liquid-crystal switches are now regarded as the most promising candidates for implementation [7].

Based on their structure and operation, MEMS switches may be further divided [16] into two-dimensional (2-D) MEMS switches and three-dimensional (3-D) MEMS switches. A 2-D switch has a crossbar structure, and this technology has the advantages of simpler fabrication, easier controllability, and a more mature technology. In this paper, we look into the

architecture of this kind of a switch. The biggest single block of 2-D MEMS switches reported so far is a 32×32 switch [17]. By itself, without applying any multistage techniques, this size is not enough for the next-generation optical network, which is expected to transmit and switch hundreds, or even thousands, of wavelengths per OXC. Even if larger scale MEMS switch blocks (e.g., 512×512 or more) are produced, other factors like high insertion loss and large insertion loss difference between calls will limit its practicability [18]. Constructing a large-scale MEMS switch in a multistage fashion seems to be the most feasible way of using this technology to construct a large switching matrix. The small-scale switch blocks can be interconnected with fibers in the way of either fiber connector or fiber splicing. We focus on the design issues involved in such a multistage switch and its performance parameters on the maximum power loss of calls and the maximum power loss difference between calls. Note that other performance parameters like crosstalk and reflection loss may also be considered for the multistage MEMS switches. For these parameters, the performance of a single MEMS switch block is generally very good. (For example, a commercially available 16×16 MEMS switch has a typical crosstalk smaller than -50 dB, and a typical reflection loss greater than 50 dB.) We may, therefore, normally ignore these effects, even for a multistage MEMS switch architecture.

The three-stage Clos network is found to be an effective and efficient architecture to build a large-scale switch [19], [20]. In this paper, we have selected this approach to construct multistage MEMS switches. To reduce the maximum power loss of calls and the maximum loss difference between calls, we also propose optimal connection patterns to connect the outlet ports and the inlet ports between the neighboring switch stages for the Clos network. These connection patterns are found to be effective enough to minimize both the maximum power loss of calls and the maximum loss difference between calls.

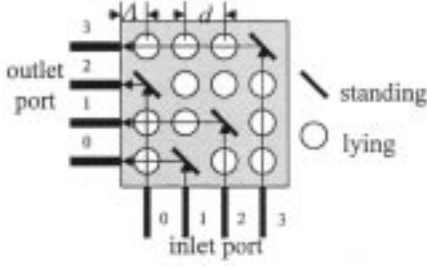
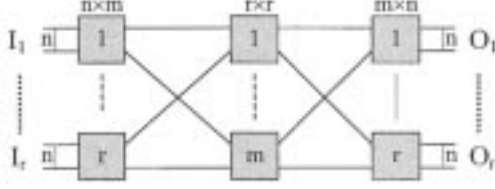
The rest of the paper is organized as follows. In Section II, we describe the operation and working principle of a 2-D MEMS optical switch and introduce the three-stage Clos switch network. In Section III, we develop a model to approximately evaluate the insertion loss of calls in a MEMS optical switch. Three efficient connection patterns used to connect the outlet ports and the inlet ports between the neighboring stages of the Clos switch are proposed in Section IV. Section V analyzes the performance results for the proposed connection patterns in terms of the maximum power loss and the maximum loss difference. We present our conclusions in Section VI.

Manuscript received 20 March, 2001; revised 30 October, 2001.

G. Shen, T. H. Cheng, C. Lu, and T. Y. Chai are with the NTRC, Nanyang Technological University, Singapore 639798, Singapore (e-mail: egxshen@ntu.edu.sg; ethcheng@ntu.edu.sg; eclu@ntu.edu.sg).

S. K. Bose is with the Department of Electrical Engineering, I. I. T. Kanpur, Kanpur 208 016, India (e-mail: skb@iitk.ac.in).

Publisher Item Identifier S 0733-8724(02)00467-X.

Fig. 1. 4×4 nonblocking in strict sense MEMS optical switch.Fig. 2. Three-stage Clos network $v(m, n, r)$.

II. 2-D MEMS OPTICAL SWITCH AND THREE-STAGE CLOS NETWORK

Fig. 1 illustrates a typical 4×4 2-D MEMS switch with four inlet ports, four outlet ports, and a total of 16 controllable micromirrors. By making the mirrors *stand up* or *lie down*, the light from any inlet port may be switched to any desired outlet port. For example, to switch the light from inlet port 3 to outlet port 3, the mirror at (3,3) is set to *stand up* to reflect the light while all of the other micromirrors in the third row and the third column must be set to *lie down*. Switches may be divided into three classes based on their call blocking characteristics, i.e., *nonblocking in strict sense*, *nonblocking in wide sense*, and *rearrangeable nonblocking* [19], [20]. The 2-D MEMS switch has a crossbar architecture, so it is *nonblocking in the strict sense*.

The three-stage Clos network $v(m, n, r)$ is shown in Fig. 2, which may be used to achieve all of the above-mentioned three kinds of switch call blocking characteristics. The following results hold.

- 1) A three-stage Clos network is *nonblocking in strict sense* if and only if $m \geq 2n - 1$ and if all of the subswitches are also *nonblocking in strict sense*.
- 2) A three-stage Clos network is rearrangeable nonblocking if and only if $m \geq n$. The subswitches may, however, be either nonblocking in strict sense or *rearrangeable nonblocking*.

III. MODELS OF INSERTION LOSS

A. Single MEMS Switch Block

The loss in a single MEMS switch block consists of four components [18]: loss due to Gaussian-beam divergence; loss due to angular misalignment; loss due to air absorption; and mirror reflection loss. The first three losses are directly related to the free-space distance between the inlet port and the outlet port and we will combine them together in a generic term called *loss due to free-space distance*. This approximation is supported by the

experimental and analysis results of [18], which shows that the loss is almost linearly increasing with propagation distance.

We develop the loss model for a single MEMS switch block. For an $n \times m$ block with n inlet ports and m outlet ports, we use the following notations:

- i index of the i th inlet port, $0 \leq i \leq n - 1$;
- j index of the j th outlet port, $0 \leq j \leq m - 1$;
- d free-space distance between two neighboring mirrors, as shown in Fig. 1;
- Λ free-space distance between an inlet (outlet) port and its neighboring mirror, as shown in Fig. 1;
- κ reflection loss of a micromirror;
- α loss coefficient due to the free-space distance;
- c connection loss between a fiber and a MEMS switch.

As shown in Fig. 1, the total loss of signal in a call transiting the switch block consists of the loss due to the free-space distance between the inlet port and the outlet port, one mirror reflection loss, and fiber connection loss. Given that a call is switched from the i th inlet port to the j th outlet port, we can express the total loss in decibels as follows:

$$L_s(i, j) = (i + j)d\alpha + 2\Lambda\alpha + \kappa + 2c. \quad (1)$$

B. Three-Stage Clos Network

Let I_i^l represent a generic inlet port of the l_i th matrix (MEMS switch block) at the i th stage, and O_i^l represent a generic outlet port of the l_i th matrix at the i th stage. For a three-stage Clos network $v(m, n, r)$, we can show that:

- a) at the first stages, $1 \leq l_1 \leq r$, $0 \leq I_1^{l_1} \leq n - 1$, and $0 \leq O_1^{l_1} \leq m - 1$;
- b) at the second stage, $1 \leq l_2 \leq m$, $0 \leq I_2^{l_2} \leq r - 1$, and $0 \leq O_2^{l_2} \leq r - 1$;
- c) at the third stage, $1 \leq l_3 \leq r$, $0 \leq I_3^{l_3} \leq m - 1$, and $0 \leq O_3^{l_3} \leq n - 1$.

The total power loss of the call in a three-stage Clos network is the sum of the losses in each of the blocks. In a Clos network, the connection pattern between inlet ports and outlet ports of two neighboring stages can be arbitrary as long as the condition of *full connection* [20] is satisfied (i.e., each matrix at the i th stage is always connected to each matrix at the $(i + 1)$ th stage by a single link). Therefore, the connection pattern is, in fact, a function of the outlet port index at the i th stage versus the inlet port index at the $(i + 1)$ th stage. Given the connection pattern p , we define this function as $I_{i+1}^{l_{i+1}} = f_p(O_i^{l_i})$ and have the loss model for a three-stage Clos network as follows:

$$\begin{aligned} L_m & \left(I_1^{l_1}, O_1^{l_1}, I_2^{l_2}, O_2^{l_2}, I_3^{l_3}, O_3^{l_3} \right) \\ & = L_m \left(I_1^{l_1}, O_1^{l_1}, f_{p_1} \left(O_1^{l_1} \right), O_2^{l_2}, f_{p_2} \left(O_2^{l_2} \right), O_3^{l_3} \right) \\ & = \left[I_1^{l_1} + O_1^{l_1} + f_{p_1} \left(O_1^{l_1} \right) + O_2^{l_2} + f_{p_2} \left(O_2^{l_2} \right) + O_3^{l_3} \right] d\alpha \\ & \quad + 6\Lambda\alpha + 3\kappa + 6c. \end{aligned} \quad (2)$$

Here, p_1 is the connection pattern existing between the first stage and the second stage and p_2 is the connection pattern existing between the second stage and the third stage.

1) *Maximum Power Loss of Calls:* For a Clos network $v(m, n, r)$ with the connection patterns p_1 and p_2 , we can use (2) to obtain the maximum power loss of calls as

$$\begin{aligned} M_m(p_1, p_2) &= \max_1 \left\{ \left[I_1^{l_1} + O_1^{l_1} + f_{p_1} \left(O_1^{l_1} \right) + O_2^{l_2} \right. \right. \\ &\quad \left. \left. + f_{p_2} \left(O_2^{l_2} \right) + O_3^{l_3} \right] d\alpha \right. \\ &\quad \left. + 6\Lambda\alpha + 3\kappa + 6c \right\} \\ &= \left[2n - 2 + \max_1 \left\{ O_1^{l_1} + f_{p_1} \left(O_1^{l_1} \right) \right\} \right. \\ &\quad \left. + \max_1 \left\{ O_2^{l_2} + f_{p_2} \left(O_2^{l_2} \right) \right\} \right] d\alpha \\ &\quad + 6\Lambda\alpha + 3\kappa + 6c \end{aligned} \quad (3)$$

where $\max_1 \{\bullet\}$ is defined as

$$\begin{aligned} \max_1 \{\bullet\} &= \max \left\{ \bullet \mid \left(0 \leq I_1^{l_1}, O_3^{l_3} \leq n - 1; \right. \right. \\ &\quad \left. \left. 0 \leq I_3^{l_3}, O_1^{l_1} \leq m - 1; \right. \right. \\ &\quad \left. \left. 0 \leq I_2^{l_2}, O_2^{l_2} \leq r - 1; \right. \right. \\ &\quad \left. \left. 1 \leq l_1, l_3 \leq r; 1 \leq l_2 \leq m \right) \right\}. \end{aligned}$$

In optical communications, it would be important to minimize the maximum power loss of the calls switched by an optical switch. Therefore, we need to find the best connection patterns p_1 and p_2 , which can minimize the maximum power loss of the calls. In a Clos network $v(m, n, r)$, there are $(m!)^r (r!)^m$ connection patterns between two neighboring stages, in which each switch in the first stage is connected exactly once to each switch in the second stage. There are a total of $(m!)^{2r} (r!)^{2m}$ such possible connection patterns for the whole network. Searching exhaustively for the optimal patterns would be very difficult even for reasonably small values of m , n , and r . Instead, trying some efficient heuristic patterns may be a more effective option. To evaluate the relative merits of the proposed heuristic patterns, it would be useful to know at least the *lower bound* on the maximum power loss of calls for all the connection patterns.

In (3), the maximum values of $O_1^{l_1} + f_{p_1} \left(O_1^{l_1} \right)$ and $O_2^{l_2} + f_{p_2} \left(O_2^{l_2} \right)$ are determined by the connection patterns used. However, for any connection patterns p_1 and p_2 , we have $\left[O_1^{l_1} + f_{p_1} \left(O_1^{l_1} \right), O_2^{l_2} + f_{p_2} \left(O_2^{l_2} \right) \right] \geq \max\{m - 1, r - 1\}$. Therefore, the *lower bound* on the maximum power loss of calls will be

$$\begin{aligned} M_m(p_1, p_2) &\geq 2 \left[n + \max\{m - 1, r - 1\} - 1 \right] d\alpha \\ &\quad + 6\Lambda\alpha + 3\kappa + 6c. \end{aligned} \quad (4)$$

2) *Maximum Loss Difference Between Calls:* Like the maximum power loss of calls, the maximum loss difference between calls would also be an important parameter in optical communications. To compute it, we first define an operator $\nabla\langle\bullet\rangle$, which gives the difference between the maximum value and the minimum value of a function. The detailed definition and properties of this operator are provided in Appendix A.

Based on the operator $\nabla\langle\bullet\rangle$, the maximum loss difference between calls in a Clos network $v(m, n, r)$ is computed as shown in (5) at the bottom of the page. Here

$$\begin{aligned} \min_1 \{\bullet\} &= \min \left\{ \bullet \mid \left(0 \leq I_1^{l_1}, O_3^{l_3} \leq n - 1 \right. \right. \\ &\quad \left. \left. 0 \leq I_3^{l_3}, O_1^{l_1} \leq m - 1 \right. \right. \\ &\quad \left. \left. 0 \leq I_2^{l_2}, O_2^{l_2} \leq r - 1 \right. \right. \\ &\quad \left. \left. 1 \leq l_1, l_3 \leq r; 1 \leq l_2 \leq m \right) \right\}. \end{aligned}$$

Note that $\min\{m - 1, r - 1\} \leq \left[O_1^{l_1} + f_{p_1} \left(O_1^{l_1} \right), O_2^{l_2} + f_{p_2} \left(O_2^{l_2} \right) \right] \leq \max\{m - 1, r - 1\}$ for any connection patterns p_1 and p_2 . With (5), therefore, we have the *lower bound* of the maximum loss difference between calls as

$$\begin{aligned} D_m(p_1, p_2) &\geq 2d\alpha \left\{ n + \max\{m - 1, r - 1\} \right. \\ &\quad \left. - \min\{m - 1, r - 1\} - 1 \right\}. \end{aligned} \quad (6)$$

IV. CONNECTION PATTERNS

A. Extended Generalized Shuffle (EGS) Connection Pattern

In a three-stage Clos network, a specific type of connection pattern, referred to as *extended generalized shuffle* (EGS), is often used to connect two neighboring switch stages. This requires that the connections between the outlets at one stage and the inlets at the next stage comply with the following relationship [20]:

$$l_{i+1} = O_i^{l_i} + 1 \text{ and } I_{i+1}^{l_{i+1}} = l_i - 1. \quad (7)$$

As an example, Fig. 3 illustrates a three-stage Clos network $v(4, 4, 3)$ based on the EGS interconnection pattern. In the generic case, we can infer by induction that for a three-stage Clos network $v(m, n, r)$ with the EGS connection pattern, the route with the maximum loss is given by

$$\begin{aligned} I_1^r &= n - 1 & O_1^r &= m - 1 & I_2^m &= r - 1 \\ O_2^m &= r - 1 & I_3^m &= m - 1q & O_3^r &= n - 1 \end{aligned}$$

and that the maximum call power loss (along this route) is

$$M_m(p_1, p_2, \text{EGS}) = 2(m + n + r - 3)d\alpha + 6\Lambda\alpha + 3\kappa + 6c. \quad (8)$$

$$\begin{aligned} D_m(p_1, p_2) &= \nabla \left\langle L_m \left(I_1^{l_1}, O_1^{l_1}, f_{p_1} \left(O_1^{l_1} \right), O_2^{l_2}, f_{p_2} \left(O_2^{l_2} \right), O_3^{l_3} \right) \right\rangle \\ &= d\alpha \left\{ 2n - 2 + \nabla \left\langle O_1^{l_1} + f_{p_1} \left(O_1^{l_1} \right) \right\rangle + \nabla \left\langle O_2^{l_2} + f_{p_2} \left(O_2^{l_2} \right) \right\rangle \right\} \\ &= d\alpha \left\{ 2n - 2 + \max_1 \left\{ O_1^{l_1} + f_{p_1} \left(O_1^{l_1} \right) \right\} - \min_1 \left\{ O_1^{l_1} + f_{p_1} \left(O_1^{l_1} \right) \right\} \right. \\ &\quad \left. + \max_1 \left\{ O_2^{l_2} + f_{p_2} \left(O_2^{l_2} \right) \right\} - \min_1 \left\{ O_2^{l_2} + f_{p_2} \left(O_2^{l_2} \right) \right\} \right\}. \end{aligned} \quad (5)$$

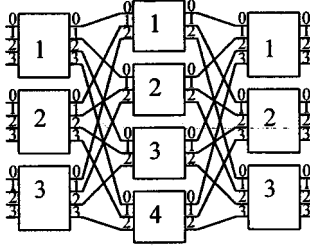


Fig. 3. A three-stage Clos network $v(4, 4, 3)$ with EGS interconnection pattern.

The route with the minimum loss is $(I_1^1 = 0, O_1^1 = 0, I_2^1 = 0, O_2^1 = 0, I_3^1 = 0, O_3^1 = 0)$ and the minimum call power loss is $6\Lambda\alpha + 3\kappa + 6c$. The maximum call loss difference is then

$$D_m(p_1, p_2, \text{EGS}) = 2(m + n + r - 3)d\alpha. \quad (9)$$

Obviously, the EGS connection pattern is not an optimal one in terms of maximum power loss of calls and maximum loss difference between calls [see (4), (6), (8), and (9)].

B. Max + Min Greedy (MMG) Connection Pattern

Intuitively, to reduce the maximum power loss of calls and the maximum loss difference between calls, we can connect the outlet ports with small indexes at one stage to the inlet ports with large indexes for the next stage. We call such types of connection patterns as Max+Min *greedy* (MMG) pattern. For example, we have illustrated this connection pattern in a step-by-step fashion in Fig. 4(a)–(d). Here, the dotted lines represent newly added connections and the solid lines represent those already added.

From this example, we can infer by induction the relationship between the outlet ports and the inlet ports at the two neighboring stages. The connection between the first stage and the second stage is given by

$$I_2^1 = \begin{cases} r - \frac{O_1^1 r + l_1}{m}, & \text{if } \frac{O_1^1 r + l_1}{m} = \text{int} \\ r - 1 - \left\lfloor \frac{O_1^1 r + l_1}{m} \right\rfloor, & \text{otherwise} \end{cases} \quad (10)$$

$$l_2 = \begin{cases} m, & \text{if } \frac{O_1^1 r + l_1}{m} = \text{int} \\ O_1^1 r + l_1 - m \left\lfloor \frac{O_1^1 r + l_1}{m} \right\rfloor, & \text{otherwise.} \end{cases} \quad (11)$$

The connection between the second stage and the third stage is given by

$$I_3^2 = \begin{cases} m - \frac{O_2^2 m + l_2}{r}, & \text{if } \frac{O_2^2 m + l_2}{r} = \text{int} \\ m - 1 - \left\lfloor \frac{O_2^2 m + l_2}{r} \right\rfloor, & \text{otherwise} \end{cases} \quad (12)$$

$$l_3 = \begin{cases} r, & \text{if } \frac{O_2^2 m + l_2}{r} = \text{int} \\ O_2^2 m + l_2 - r \left\lfloor \frac{O_2^2 m + l_2}{r} \right\rfloor, & \text{otherwise.} \end{cases} \quad (13)$$

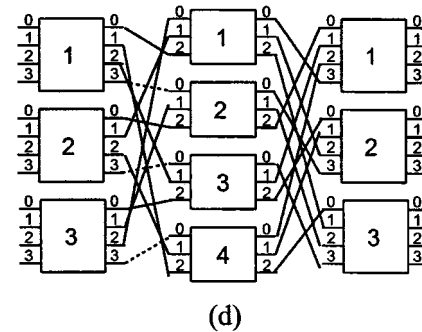
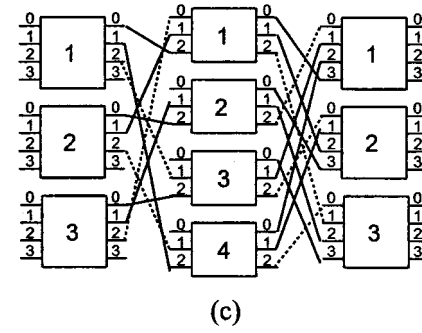
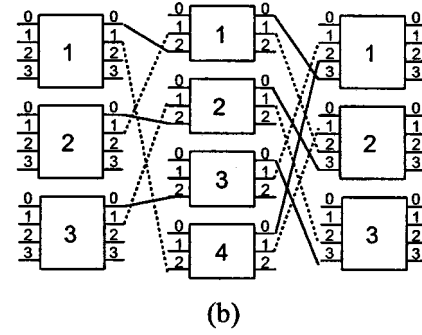
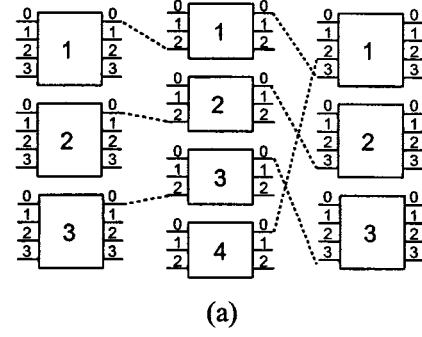


Fig. 4. An example of MMG connection pattern.

A Clos network requires the interconnection between two neighboring stages to be *fully connected*. We can show that, in order to support full connectivity in a Clos network based on the MMG pattern, the number of matrices in the neighboring stages must not share a common factor. This will now be formally stated as a theorem.

Theorem 1: The MMG connection pattern guarantees full connection between the two neighboring stages if and only if r_i and r_{i+1} do not share a common factor, where r_i and r_{i+1} are the respective numbers of the matrices at the i th and $(i+1)$ th stages.

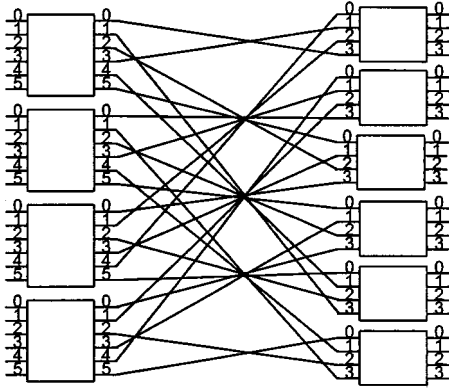


Fig. 5. The connection between neighboring stages based on MMG pattern.

We replace the terms $f_{p_1}(O_1^{l_1})$ and $f_{p_2}(O_2^{l_2})$ in the maximum power loss of (3) with (10) and (12). We get that for the following four cases:

- i) $(O_1^{l_1}r + l_1)/m \neq \text{int}$ and $(O_2^{l_2}m + l_2)/r \neq \text{int}$;
 - ii) $(O_1^{l_1}r + l_1)/m = \text{int}$ and $(O_2^{l_2}m + l_2)/r \neq \text{int}$;
 - iii) $(O_1^{l_1}r + l_1)/m \neq \text{int}$ and $(O_2^{l_2}m + l_2)/r = \text{int}$;
 - iv) $(O_1^{l_1}r + l_1)/m = \text{int}$ and $(O_2^{l_2}m + l_2)/r = \text{int}$;
- and

$$M_m(p_1, p_2, \text{MMG}) = 2[n + \max\{m - 1, r - 1\} - 1]d\alpha + 6\Lambda\alpha + 3\kappa + 6c, \quad m \neq r.$$

This is the *lower bound of maximum power loss of calls*. Here, m cannot be equal to r because they do not share any common factor.

Similarly, for the maximum loss difference between calls with the MMG connection pattern, we replace the terms $f_{p_1}(O_1^{l_1})$ and $f_{p_2}(O_2^{l_2})$ in (4) with (10) and (12), and get the result for the cases (i)–(iv) as

$$D_m(p_1, p_2, \text{MMG}) = 2d\alpha \left\{ n + \max\{m - 1, r - 1\} - \min\{m - 1, r - 1\} - 1 \right\}, \quad m \neq r.$$

This is the *lower bound of maximum loss difference between calls*.

Therefore, we can conclude that MMG pattern is an optimal pattern because it can guarantee the Clos network to simultaneously achieve the lower bounds on both the maximum power loss of calls and the maximum loss difference between calls.

C. Compressed EGS (C-EGS) Connection Pattern

The MMG pattern cannot be used when the numbers of matrices of two neighboring stages do share a common factor, because then one cannot satisfy the requirement of *full connection* in the Clos network. An example of this is shown in Fig. 5 for two stages connected in the MMG pattern, where the first and second stages have four and six matrices, respectively (with a common factor of two). We can observe that the connection between the two stages is not a *full connection*, because there are

two connections existing at the same time between two matrices each at the two neighboring stages. Some technique other than MMG is required to handle this situation. This may be further subdivided into two cases, first, when the number in one stage is a multiple of the other, and second, when they are not multiples of each other but share a common factor.

1) *C-EGS-1: Multiple Relationship Between the Numbers of the Matrices at the Two Stages*: Consider two neighboring stages with r_1 and r_2 matrices, respectively, where $r_2 = kr_1$, ($k \geq 1$) \cap ($k = \text{int}$). (Note that for the case where r_1 is a multiple of r_2 , we can interchange the positions of the two stages and continue as shown here.) We give a proposed optimal connection pattern for this case using three steps. These steps are illustrated using the example of Fig. 6. Fig. 6(a) shows the initial connection state between the two neighboring stages based on the EGS connection pattern. The first stage has $r_1 = 3$ 6×6 matrices, whereas the second stage has $r_2 = 6$ 3×3 matrices (multiple = $k = 2$).

The three steps of the proposed procedure are as follows.

Step 1) For each matrix at the first stage, we combine k (in the example, $k = 2$) neighboring outlet ports together into one outlet port. We call this a *combined outlet port* (although it still has k real ports). Thus, the original $r_2 \times r_2$ (i.e., 6×6) matrix changes into a $r_1 \times r_1$ (i.e., 3×3) matrix. For matrices at the second stage, we combine k ($= 2$) $r_1 \times r_1$ neighboring matrices together into one matrix (this matrix consists of k real matrices), which we call a *combined matrix*. Based on these combinations, the network is now compressed into a symmetric matrix, as shown in Fig. 6(b).

Step 2) Based on the network obtained in Step 1), modify the indexes of the outlet ports at the first stage and the inlet ports at the second stage. Assume $(O_0, O_1, \dots, O_{r_1-1} = 0, 1, \dots, r_1 - 1)$ is the initial index sequence of the outlet port of each matrix at the first stage [e.g., the sequence (0, 1, 2), as shown in Fig. 6(b)]. We implement various left-circulating shift operations on these index sequences as follows. For the first matrix, its index sequence is kept same as its initial format. For the second matrix, we left circulate its sequence by one index, e.g., the new sequence is (1, 2, 0), as shown in Fig. 6(c). In the general case, for the r_1 th matrix, we left circulate the sequence by $r_1 - 1$ indexes, starting from the initial index sequence, e.g., the new sequence is (2, 0, 1), as shown in Fig. 6(c). Similar operation is implemented for the matrices in the second stage. Assuming that $(I_0, I_1, \dots, I_{r_1-1} = 0, 1, \dots, r_1 - 1)$ is the initial index sequence of the inlet port of each matrix at the second stage [e.g., the sequence (0, 1, 2), as shown in Fig. 6(b)], we implement the following operations. For the first matrix, we reverse its index sequence [e.g., the sequence changes to (2, 1, 0), as shown in Fig. 6(c)]. For the second matrix, based on the reversed sequence, we left circulate it by one index [e.g., it now changes into the sequence (1, 0,

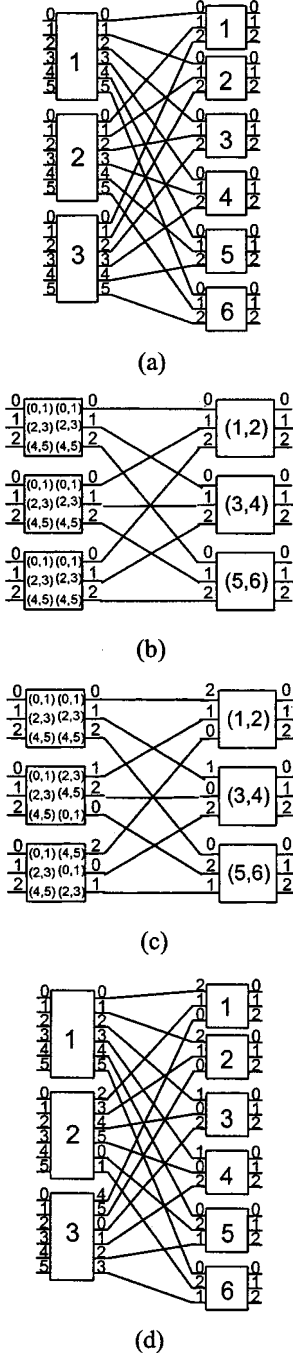


Fig. 6. An example of C-EGS-1 connection pattern.

2), as shown in Fig. 6(c)]. In general, for the r_1 th matrix, we left circulate the initial reversed index sequence by $r_1 - 1$ indexes [e.g., the new sequence changes into (0, 2, 1) as shown in Fig. 6(c)]. Note that during this operation, the connection links between two neighboring stages are kept the same at all times.

Step 3) Based on Step 2), we extend (uncompress) the *combined ports* and the *combined matrices* so as to find the real connection pattern between two neighboring stages without the compression. We connect each real outlet port in each *combined port* to one of real matrices in the *combined matrix*, which is connected

with the *combined port* in the compressed network. The final extended real connections for the example are shown in Fig. 6(d).

Because the connection pattern of the compressed network with the *combined ports* and the *combined matrices* is the EGS pattern, this network is a *full connection* network. In addition, the number of real ports in each *combined port* is the same as that of real matrices in its corresponding *combined matrix*, which requires that only one real port connects to a real matrix. Therefore, the new connection pattern C-EGS-1 is a *full connection* pattern.

We obtained our final connection pattern based on the EGS pattern by various rotation and reversing operations. Therefore, the mathematical relationship for the proposed pattern can also be derived from that of EGS pattern. Starting from (7), we infer by induction the relationship of the connections for the compressed network, whose notations are marked with the prime symbol ($'$), as follows:

$$l'_{i+1} = \begin{cases} O_i^{l'_i} - l'_i + 2, & \text{if } O_i^{l'_i} \geq l'_i - 1 \\ r'_i - l'_i + O_i^{l'_i} + 2, & \text{if } O_i^{l'_i} < l'_i - 1 \end{cases} \quad (14)$$

$$I'_{i+1} = \begin{cases} r'_{i+1} - l'_{i+1} - l'_i + 1, & \text{if } O_i^{l'_i} \geq l'_i - 1 \\ 2r'_{i+1} - l'_{i+1} - l'_i + 1, & \text{if } O_i^{l'_i} < l'_i - 1. \end{cases} \quad (15)$$

As described earlier, each real outlet port in each *combined port* is connected to one of real matrices in the *combined matrix*, which is connected with the *combined port* in the compressed network. We describe these connections in mathematical format as follows.

The real outlet ports at the first stage, whose indexes are within the set

$$O_i^{l'_i} \in [kO_i^{l'_i}, k(O_i^{l'_i} + 1) - 1] \quad (16)$$

are arbitrarily connected to the inlet ports, whose index is

$$I_{i+1}^{l'_{i+1}} = I'_{i+1} \quad (17)$$

on the matrices, whose indexes are within the set

$$l_{i+1} \in [(l'_{i+1} - 1)k + 1, kl'_{i+1}] \quad (18)$$

at the second stage.

Here, the notations without prime symbol ($'$) are used to denote the terms corresponding to the real ports and matrices, and k is the multiple between the numbers of matrices at the two neighboring stages, i.e., $k = r_{i+1}/r_i$ and $O_i^{l'_i} \in [0, r_i - 1]$.

2) *Maximum Power Loss of Calls and the Maximum Loss Difference Between Calls*: For a Clos network, given that the number of matrices at the second stage r_2 is a multiple of that of matrices at the first or the third stage r_1 and r_3 , ($r_1 = r_3$); we connect any two neighboring stages based on the C-EGS-1

connection pattern. For the maximum power loss of calls, we have

$$M_m(p_1, p_2, \text{C-EGS-1}) = (2n-2)d\alpha + \max_1 \left\{ O_1^{l_1} + I_2^{l_2} \right\} \\ + \max_1 \left\{ O_2^{l_2} + I_3^{l_3} \right\} + 6\Lambda\alpha + 3\kappa + 6c.$$

Based on (14) and (15), we get $O_i^{l_i} + I_{i+1}^{l_{i+1}} = r'_{i+1} - 1 = r'_i - 1 = r_i - 1$.

We then select the maximum value $O_1^{l_1} = k(O_1^{l_1} + 1) - 1$ from the set given by (16), and further have that

$$\max_1 \left\{ O_1^{l_1} + I_2^{l_2} \right\} = \max_2 \left\{ I_2^{l_2} + k(O_1^{l_1} + 1) - 1 \right\} \\ = \max_2 \left\{ I_2^{l_2} + O_1^{l_1} + (k-1)(O_1^{l_1} + 1) \right\} \\ = r_1 - 1 + \left(\frac{r_2}{r_1} - 1 \right) r_1 = r_2 - 1.$$

Here

$$\max_2 \{ \bullet \} = \max \left\{ \bullet \mid \left(0 \leq O_1^{l_1}, O_2^{l_2}, I_2^{l_2}, I_3^{l_3} \leq r_1 - 1; \right. \right. \\ \left. \left. 1 \leq l_1, l_2, l_3 \leq r_1 \right) \right\}.$$

Similarly, we also have that $\max_1 \left\{ O_2^{l_2} + I_3^{l_3} \right\} = r_2 - 1$. Therefore, the maximum power loss of calls is

$$M_m(p_1, p_2, \text{C-EGS-1}) = 2(n + r_2 - 2)d\alpha \\ + 6\Lambda\alpha + 3\kappa + 6c. \quad (19)$$

This is equal to the *lower bound of maximum power loss of calls*.

For the maximum loss difference between calls, we can select any outlet port index from the set of (16), and put it in (5). If we select the minimum inlet port index, then

$$D_m(p_1, p_2, \text{C-EGS-1}) \\ = d\alpha \left\{ 2n - 2 + \nabla \left\langle I_2^{l_2} + O_1^{l_1} + (k-1)O_1^{l_1} \right\rangle \right. \\ \left. + \nabla \left\langle I_3^{l_3} + O_2^{l_2} + (k-1)O_2^{l_2} \right\rangle + 2(k-1) \right\} \\ = 2d\alpha [n + r_2 - r_1 - 1]. \quad (20)$$

This is equal to the *lower bound of maximum loss difference between calls*. In each *combined outlet port*, there can be a difference up to $(k-1)$ in the indexes of its real outlet ports, so to calculate the maximum loss difference, we need to add this value in the equation.

For the case that the number of matrices at the first and the third stages are both a multiple of that of the matrices at the second stage, we can use the same connection pattern to get the same results as those in (19) and (20). Therefore, we can conclude, in general, that the C-EGS-1 connection pattern is an optimal one.

3) *C-EGS-2: Common Factor Only Between the Numbers of the Matrices at the Two Stages:* We now consider the case

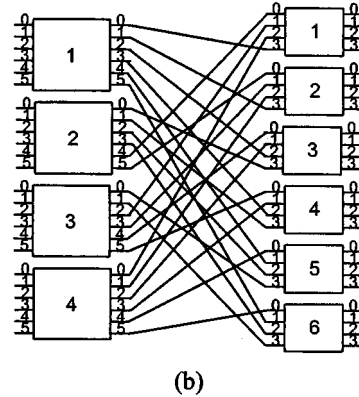
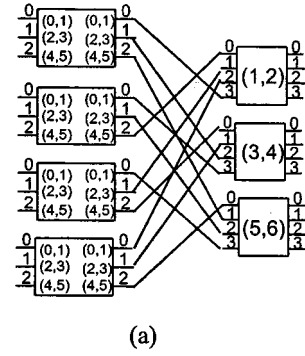


Fig. 7. An example of C-EGS-2 connection pattern.

where the numbers of matrices in the two neighboring stages share a common factor, but one is not a multiple of the other. Assume there are r_1 matrices in the first stage, and r_2 matrices in the second stage. Assume that r_2 is greater than r_1 , and that they have the maximum common factor k , which we denote as $c(r_1, r_2)$. We compress the network by the factor k . After compression, we get a network where the number of matrices at each stage do not share a common factor. Therefore, for the compressed network, we may apply the MMG connection pattern to connect the ports at the two neighboring stages. The connection pattern developed based on this is referred to as the C-EGS-2 connection pattern.

In Fig. 7, we consider an example illustrating the steps in constructing this connection pattern. Initially, assume that there are two stages: the first stage has four 6×6 matrices, and the second stage has six 4×4 matrices. Here, $c(4, 6) = 2$ and, therefore, two real outlet ports and two real matrices will form a *combined port* and a *combined matrix*, respectively. The MMG connection pattern is applied to the compressed network. Fig. 7(a) shows the compressed network with the MMG connection pattern. Finally, based on the connections in the compressed network, we extend them back to the connections between those real ports. Fig. 7(b) shows the result after this final step.

The compressed connection pattern shown in Fig. 7(a) is a *full connection* pattern because it is connected based on MMG pattern. In addition, the number of real outlet ports in each *combined outlet port*, k , is equal to that of real matrices in each *combined matrix*, so each real outlet port is connected to a different real matrix. Based on these, we can, therefore, conclude that the

TABLE I
PERFORMANCE RESULTS FOR THE THREE-STAGE CLOS NETWORK $v(m, n, r)$, $\sigma = 6\Lambda\alpha + 3\kappa + 6c$

	Single crossbar block	EGS	MMG	C-EGS-1 ($m=kr$ or $r=km$)	C-EGS-2 [$c(m,r)=k$, but $k \neq m$ or r]
Low bound of the maximum loss	$2[n + \max\{m-1, r-1\} - 1]d\alpha + \sigma$				
Low bound of the maximum loss difference	$2d\alpha\{n + \max\{m-1, r-1\} - \min\{m-1, r-1\} - 1\}$				
Maximum loss	$2(nr-1)d\alpha + 2\Lambda\alpha + \kappa + 2c$	$2(m+n+r-3)d\alpha + \sigma$	Low bound of the maximum loss		
Maximum loss difference	$2(nr-1)d\alpha$	$2(m+n+r-3)d\alpha$	Low bound of the maximum loss difference		
Total number of mirrors	$n^2 r^2$	$mr(2n+r)$			

C-EGS-2 connection pattern can also guarantee the requirement of *full connection* in a Clos network.

We use the notation marked with the symbol ($'$) to denote the *combined ports* and *combined matrices*. We can then write the general expressions of the MMG connection pattern for the compressed network, as shown in (21) and (22).

$$I_{i+1}' = \begin{cases} r_i' - \frac{O_i' r_i' + l_i'}{r_{i+1}'}, & \text{if } \frac{O_i' r_i' + l_i'}{r_{i+1}'} = \text{int} \\ r_i' - 1 - \left\lfloor \frac{O_i' r_i' + l_i'}{r_{i+1}'} \right\rfloor, & \text{otherwise.} \end{cases} \quad (21)$$

$$l_{i+1}' = \begin{cases} r_{i+1}', & \text{if } \frac{O_i' r_i' + l_i'}{r_{i+1}'} = \text{int} \\ O_i' r_i' + l_i' - r_{i+1}' \left\lfloor \frac{O_i' r_i' + l_i'}{r_{i+1}'} \right\rfloor, & \text{otherwise.} \end{cases} \quad (22)$$

Note that, here, $r_i' = r_i$ and $r_{i+1}' = r_{i+1}/k$. After extending the connections, we can describe the connections in mathematical format for the real network in the same fashion as that of C-EGS-1 [see (16)–(18)].

4) *Maximum Power Loss of Calls and the Maximum Loss Difference Between Calls*: Consider a Clos network where the number of matrices at the second stage is r_2 and the numbers at each of the first and the third stages are r_1 and r_3 ($r_1 = r_3$), where r_2 is assumed to be greater than r_1 (or r_3). We assume, further, that between r_2 and r_1 (or r_3), there is the maximum common factor $c(r_1, r_2) = c(r_2, r_3) = k$, but that r_2 is not a multiple of r_1 (or r_3). We connect any two neighboring stages based on the C-EGS-2 connection pattern. For the maximum power loss of calls, we have that

$$M_m(p_1, p_2, \text{C-EGS-2}) = (2n-2)d\alpha + \max_1 \left\{ O_1^{l_1} + I_2^{l_2} \right\} + \max_1 \left\{ O_2^{l_2} + I_3^{l_3} \right\} + 6\Lambda\alpha + 3\kappa + 6c.$$

Using (21), we can get that

$$\max_1 \left\{ O_1^{l_1} + I_2^{l_2} \right\} = \max_2 \left\{ I_2^{l_2} + k \left(O_1^{l_1} + 1 \right) - 1 \right\} = r_2 - 1.$$

Similarly, we also have that $\max_1 \left\{ O_2^{l_2} + I_3^{l_3} \right\} = r_2 - 1$.

Using these, we get

$$M_m(p_1, p_2, \text{C-EGS-2}) = 2(n+r_2-2)d\alpha + 6\Lambda\alpha + 3\kappa + 6c \quad (23)$$

as the *lower bound of maximum power loss of calls*.

For the maximum loss difference between calls, we also can select any outlet port index from the set (16) and put it in (5). Selecting the minimum inlet port index, we can then get

$$D_m(p_1, p_2, \text{C-EGS-2}) = d\alpha \left\{ 2n - 2 + \nabla \left\langle I_2^{l_2} + kO_1^{l_1} \right\rangle + \nabla \left\langle I_3^{l_3} + kO_2^{l_2} \right\rangle + 2(k-1) \right\} = 2d\alpha [n + r_2 - r_1 - 1] \quad (24)$$

as the *lower bound of maximum loss difference between calls*.

Therefore, based on (23) and (24), we conclude that the connection pattern C-EGS-2 is also an optimal pattern in terms of the maximum loss of calls and the maximum loss difference between calls.

V. PERFORMANCE RESULTS AND DISCUSSION

We apply the proposed connection patterns to the Clos network $v(m, n, r)$ and the corresponding performance results are listed in Table I for purposes of comparison.

From Table I, we can find that compared to a single block MEMS switch of the same scale, a three-stage Clos network has the advantages of lower maximum power loss of calls and lower maximum loss difference between calls, and needs fewer micromirrors to construct the switch. We also observe that a Clos network based on an EGS connection pattern does not have an optimal performance. This is true even though the EGS connection pattern has been widely employed to connect two neighboring stages in traditional Clos networks. Our proposed new connection patterns show very good performances in terms of both the maximum power loss of calls and the maximum loss difference between calls because these are both small enough to reach their respective *lower bounds*. Moreover, the proposed connection patterns are versatile enough to deal with all kinds of

Clos network cases. These include when m and r do not share a common factor, when m and r share a common factor but one is not the multiple of the other, and when m and r are a multiple of each other (i.e., $m = kr$ or $r = km$).

A. Rearrangeable Nonblocking Network ($m = n$)

Consider the micromirror requirement of an $N \times N$ rearrangeable nonblocking Clos network of the type where the first and the last stages have $n = \sqrt{N/2}$, and the second stage has $r = \sqrt{2N}$. The proposed optimal networks require $2N\sqrt{2N}$ micromirrors,¹ which would be much smaller than the N^2 required by a crossbar MEMS block when N is large (e.g., $N \geq 8$).

On the maximum power loss of calls, note that when $n \geq r$, the lower bound on the maximum power loss of calls in a Clos network is $4(n-1)d\alpha + \sigma$. Similarly, when $n \leq r$, the lower bound on the maximum power loss has the minimum value² $4(\sqrt{N}-1)d\alpha + \sigma$ when $n = r = \sqrt{N}$. We can, therefore, conclude that the minimum of the low bound of the maximum power loss for an $N \times N$ rearrangeable nonblocking Clos network is $4(\sqrt{N}-1)d\alpha + \sigma$ when $n = r = \sqrt{N}$.

Finally, on the maximum loss difference between calls, we find that for a rearrangeable nonblocking Clos network when $n = r$, the lower bound of the maximum loss difference between calls becomes the minimum, $2(n-1)d\alpha$. This is actually equal to the maximum loss difference between calls of an $n \times n$ single MEMS switch block. This means that with the proposed optimal connection patterns, a rearrangeable nonblocking Clos network can have the same loss difference between calls as that of a single MEMS switch block, which is used to construct the Clos network, although the Clos network is n or r times larger in scale than the single block switch.

From this, we can conclude that in order to construct an $N \times N$ rearrangeable nonblocking Clos switch, a three-stage Clos network with $\sqrt{N} \sqrt{N} \times \sqrt{N}$ MEMS blocks at each stage may be used. This will have the best performance in terms of both the maximum power loss of calls and the maximum loss difference between calls over the whole set of permutations (n, r) . Moreover, the total number of micromirrors required by this kind of network is $3N\sqrt{N}$, which is very close to the lower bound on the number of mirrors required by a rearrangeable nonblocking $N \times N$ Clos switch (i.e., $2\sqrt{2}N\sqrt{N} \cong 2.828N\sqrt{N}$).

B. Strictly Nonblocking Network ($m = 2n - 1$)

An $N \times N$ strictly nonblocking Clos network where the scale of the blocks³ is $n \cong \sqrt{N/2}$ requires a minimum total number of micromirrors equal to $4\sqrt{2}N^{3/2} - 4N$. For large N , this is much smaller than N^2 , which would be required by a crossbar MEMS block.

When $2n - 1 \geq r$, the lower bound on the maximum power loss of calls in a Clos network is $6(n-1)d\alpha + \sigma$, and when $2n - 1 \leq r$, the lower bound on the maximum power loss has

¹ $2n^2r + nr^2 = N(2n + N/n) \geq 2N\sqrt{2N}$, when $n = \sqrt{N/2}$, $r = \sqrt{2N}$.
² $2(n+r-2)d\alpha + \sigma = 2(N/r + r - 2)d\alpha + \sigma \geq 4(\sqrt{N}-1)d\alpha + \sigma$, when $r = n = \sqrt{N}$.

³ $(2n-1)r(2n+r) = 4Nn + 2N^2/n - 2N - N^2/n^2 \cong 4Nn + 2N^2/n - 2N \geq 4\sqrt{2}N^{3/2} - 2N$, when $n = \sqrt{N/2}$.

the minimum⁴ $6(\sqrt{N/2}-1)d\alpha + \sigma$. Therefore, in the whole set of permutations (n, r) , it is found that when $n \cong \sqrt{N/2}$ (i.e., $r \cong \sqrt{2N}$), the minimum of the maximum power loss of calls is about $6(\sqrt{N/2}-1)d\alpha + \sigma$.

Finally, on the maximum loss difference between calls, we find that for a rearrangeable nonblocking Clos network with $2n - 1 = r$, (i.e., $n \cong \sqrt{N/2}$), the lower bound on the maximum loss difference between calls is the minimum, $2(\sqrt{N/2}-1)d\alpha$. Note that this is actually similar to the maximum loss difference between calls of a single $n \times n$ MEMS switch block.

From this, we conclude that to construct an $N \times N$ strictly nonblocking Clos switch, a three-stage Clos network with $\sqrt{2N} \sqrt{N/2} \times (\sqrt{2N}-1)$ MEMS blocks at the first and the third stages, and $\sqrt{2N}-1 \sqrt{2N} \times \sqrt{2N}$ MEMS blocks at the second stage, should be used. This would show the best performance in the terms of both the maximum power loss of calls and the maximum loss difference between calls in the whole set of permutations (n, r) . Moreover, the total number of micromirrors required by this kind of network is $4\sqrt{2}N^{3/2} - 4N$, which is equal to the lower bound on the number of mirrors required by a strictly nonblocking $N \times N$ Clos switch.

We have developed above the loss models and optimal connection patterns for a MEMS-based Clos switch network. It should be noted that, with minor modifications, these models and connection patterns are general enough to be applied even to the bubble-jet switch [10] or to other power loss related switches.

VI. CONCLUSION

We have considered the construction of a multistage MEMS switch network with single MEMS switch blocks. A power loss model has been developed for calls on a single MEMS block that has then been used to develop the model for a three-stage Clos network. An appropriate model for the maximum loss difference between calls has also been proposed. The paper also proposes three connection patterns (MMG, C-EGS-1, and C-EGS-2) to connect outlet ports and inlet ports between two neighboring stages in a three-stage Clos network. These connection patterns are proved to be optimal and efficient enough to reach the minimums of both the maximum power loss of calls and the maximum loss difference between calls.

APPENDIX

Definition: For $\forall g(x_1, x_2, \dots, x_n)$ with the variables x_1, x_2, \dots, x_n , define $\nabla\langle\bullet\rangle$ as

$$\begin{aligned} \nabla\langle g(x_1, x_2, \dots, x_n) \rangle \\ \triangleq \max \{g(x_1, x_2, \dots, x_n) | x_1, x_2, \dots, x_n\} \\ - \min \{g(x_1, x_2, \dots, x_n) | x_1, x_2, \dots, x_n\}. \end{aligned}$$

This operator has the following properties.

- 1) $\nabla\langle c \rangle = 0$ if c is a constant.

⁴Approximately $2n - 1 \leq r \Rightarrow r^2 + r - 2N \geq 0 \Rightarrow r \geq \sqrt{2N}$; $2n - 1 \leq r \Rightarrow 2n^2 - n - N \leq 0 \Rightarrow n \leq \sqrt{N/2}$.

- 2) $\nabla \langle g(x_1, x_2, \dots, x_n) \rangle = \nabla \langle -g(x_1, x_2, \dots, x_n) \rangle$. As a special case, $\nabla \langle x \rangle = \nabla \langle -x \rangle$.
- 3) $\nabla \langle ag(x_1, x_2, \dots, x_n) \rangle = a \nabla \langle g(x_1, x_2, \dots, x_n) \rangle$.
- 4) If $g(x_1, x_2, \dots, x_n) = a_1 g_1(x_1) \pm a_2 g_2(x_2) \pm \dots \pm a_n g_n(x_n)$, then $\nabla \langle g(x_1, x_2, \dots, x_n) \rangle = a_1 \nabla \langle g(x_1) \rangle + a_2 \nabla \langle g(x_2) \rangle + \dots + a_n \nabla \langle g(x_n) \rangle$. As a special case, $\nabla \langle ax \pm by \rangle = a \nabla \langle x \rangle + b \nabla \langle y \rangle$.

REFERENCES

- [1] R. Bala, J. Luciani, and D. Awduche *et al.*, "IP over optical networks: A framework," Internet draft, draft-many-ip-optical-framework-03.txt, work in progress [Online].
- [2] N. Chandhok, A. Durresti, and R. Jagannathan *et al.*, "IP over optical networks: A summary of issues," Internet draft, draft-osu-ipo-mpls-issues-02.txt, work in progress [Online].
- [3] D. Awduche, Y. Rekhter, J. Drake, and R. Coltun, "Multi-protocol lambda switching: Combining MPLS traffic engineering control with optical cross connects," Internet draft, draft-awduche-mpls-te-optical-03.txt, work in progress [Online].
- [4] L. Y. Lin, E. L. Goldstein, and R. W. Tkach, "Free-space micromachined optical switches with submillisecond switching time for large-scale optical crossconnects," *IEEE Photon. Technol. Lett.*, vol. 10, pp. 525–527, Apr. 1998.
- [5] L. Y. Lin, "Free-space micromachined optical-switching technologies and architectures," in *Proc. OFC'99*, vol. 2, 1999, pp. 154–156.
- [6] L. Y. Lin, E. L. Goldstein, J. M. Simmons, and R. W. Tkach, "High-density micromachined polygon optical crossconnects exploiting network connection symmetry," *IEEE Photon. Technol. Lett.*, vol. 10, pp. 1425–1427, Oct. 1998.
- [7] A. Ware, "New photonic-switching technology for all-optical networks," *Lightwave*, pp. 92–98, Mar. 2000.
- [8] M. Makihara, M. Sato, F. Shimokawa, and Y. Nishida, "Micromechanical optical switches based on thermocapillary integrated in waveguide substrate," *J. Lightwave Technol.*, vol. 17, pp. 14–18, Jan. 1999.
- [9] Light Reading. (2000) News Analysis: "Alcatel Backs the Bubbles". [Online]. Available: http://www.lightreading.com/document.asp?doc_id=1315
- [10] S. Hardy, "Liquid-crystal technology vies for switching applications," *Lightwave*, pp. 44–46, Dec. 1999.
- [11] N. K. Shankar, J. A. Morris, C. P. Yakymyshyn, and C. R. Pollock, "A 2*2 fiber optic switch using chiral liquid crystals," *IEEE Photon. Technol. Lett.*, vol. 2, pp. 147–149, Feb. 1990.
- [12] H. Lausen *et al.*, "Pigtailed thermal optic 1 x 2—Switch in polymer: Design and experimental evaluation," in *Proc. Eur. Fiber Optic Conf. Networks*, 1994, pp. 99–101.
- [13] D. K. Cheng, Y. Liu, and G. J. Sonek, "Optical switch based on thermally-activated dye-doped biomolecular thin films," *IEEE Photon. Technol. Lett.*, vol. 7, pp. 366–369, Apr. 1995.
- [14] A. Kar-Roy and C. S. Tsai, "8*8 symmetric nonblocking integrated acoustooptic space switch module on LiNbO₃," *IEEE Photon. Technol. Lett.*, vol. 7, pp. 731–734, July 1992.
- [15] D. A. Smith, A. Alessandro, J. E. Baran, D. J. Fritz, J. L. Jackel, and R. S. Chakravarthy, "Multiwavelength performance of an apodized acoustooptic switch," *J. Lightwave Technol.*, vol. 14, pp. 2044–2051, Sept. 1996.
- [16] S. Hardy, "All-optical-switching groundswell builds," *Lightwave*, pp. 45–47, May 2000.
- [17] Light Reading. (2000) Optical Switching Fabric. [Online]. Available: http://www.lightreading.com/document.asp?doc_id=2254
- [18] L. Y. Lin, E. L. Goldstein, and R. W. Tkach, "On the expandability of free-space micromachined optical cross connects," *J. Lightwave Technol.*, vol. 18, pp. 482–489, Apr. 2000.
- [19] V. E. Benes, *Mathematical Theory of Connection Networks and Telephone Traffic*. New York: Academic, 1965.
- [20] A. Pattavina, *Switching Theory: Architecture and Performance in Broadband ATM Networks*. New York: Wiley, 1998.

Gangxiang Shen (S'98–M'99), photograph and biography not available at the time of publication.

Tee Hiang Cheng (S'91–M'91), photograph and biography not available at the time of publication.

Sanjay K. Bose (SM'91), photograph and biography not available at the time of publication.

Chao Lu (M'91), photograph and biography not available at the time of publication.

Teck Yoong Chai, photograph and biography not available at the time of publication.